

# Factors affecting the estimation of GPS receiver instrumental biases

S. Kao, Y. Tu\*, W. Chen, D. J. Weng and S. Y. Ji

Global positioning system (GPS) has been widely used to investigate the ionosphere through the estimation of the total electron content (TEC) and its distributions in space. One of the important factors affecting the ionosphere TEC estimation accuracy is the hardware differential code biases (DCBs) inherited in both GPS satellites and receivers. This paper investigates various factors affecting GPS receiver instrumental bias estimation accuracy. Through a number of designed tests, we concluded that the most important factor is the ionosphere model accuracy. Some of large daily bias variations of receiver DCB detected by other studies, such as receivers in low latitude regions, are not due to the DCB changes, but the estimation errors. The DCB estimation values can vary significantly for different ionospheric models and different sizes of networks. For example, the receiver DCB values obtained from the global and the station-specific models exhibit difference from  $-2.5$  to  $14.3$  TECU for different stations. Different data processing methods also contribute to DCB estimation errors. The results from smoothing and non-smoothing GPS observation show that the difference of DCB reaches up to  $6.8$  TECU for some stations, with the mean difference of  $3$  TECU. On the other hand, the elevation cut-off angle does not play an important role in ionospheric delay estimation. For elevation cut-off angles from  $10$  to  $30^\circ$ , our tests show that the DCB estimation differences are  $<0.4$  TECU.

**Keywords:** Total electron content, differential code biases, inter-frequency biases, GPS, Ionosphere

## Introduction

Understanding ionosphere activities is important for space exploration and satellite navigation. Since late 1980s, global positioning system (GPS) has become an important tool to study global and regional ionosphere activities, through the estimation of total electron content (TEC) in space and its variations. Owing to the extensive distribution of GPS receivers in the world, the global ionosphere and variation maps have been routinely produced [9]. The precise global (or regional) ionosphere TEC models are crucial for satellite navigation and provide an important source for space weather study [6].

One of the main problems affecting TEC estimation accuracy with GPS measurements is the hardware differential code biases (DCB) inherited in both GPS satellites and receivers [5],[14]. The DCB (also called as inter-frequency biases) is caused by the relative travel times between the L1 and L2 signals from the GPS antenna to the master CPU. Since these biases are frequency dependent, they could not be removed by subtracting different frequency observations [13], [11]. The DCB must be estimated accurately and removed

from GPS measurements to achieve a reliable TEC estimation. However, it is not easy to separate the biases from the ionospheric TEC and noise items, due to its correlation with ionosphere delay parameter. Compared with GPS receiver DCB, GPS satellite DCB is relatively stable [15], and therefore is relatively easier to be estimated. Now, the precise satellite DCB estimation for each active satellite is provided by the International GNSS Service (IGS), through the analysis of a global GPS network [9]. The receiver DCB can be constant over several days under a rather smooth ionospheric behaviour. But in certain areas with great ionosphere variations such as equatorial or auroral zones, the constant assumption could not always be true [14], [11]. Various techniques have been developed to estimate GPS receiver DCB. The simplest method is to assume that TEC is never negative, and to align receiver DCB to let the nighttime vertical TEC values be in the range of  $1-3$  TECU. One TECU equals to  $10^{16} \text{ e m}^{-2}$ , which is equivalent to  $0.16$  m on GPS L1 delay. The most accurate method to determine GPS receiver DCB is to directly measure the receiver DCB using a GPS signal simulator. With this method, the DCB estimation accuracy can reach  $0.1$  TECU [8]. However, this method requires special equipment to calibrate every receiver in the network frequently which is not convenient for routine GPS ionosphere monitoring. Another method utilises the conjunctions of two

---

Department of Civil Engineering, National Chung Hsing University, 250 Kuo Kuang Road, Taichung, Taiwan

\*Corresponding author, email tuym@ntit.edu.tw

satellites passing at the same ionospheric pierce point (IPP). Then the receiver DCB can be estimated by assuming the vertical TEC observed from two satellites to be equal [10]. The most commonly used method for estimating receiver DCB is to solve the receiver DCB and ionosphere model parameters together [5], [11]. With this method, TEC spatial distribution is described as an empirical function with undetermined parameters. Using dual frequency GPS data, these model parameters and DCB can be estimated at the same time.

As the hardware DCB errors are the major source in GPS ionosphere TEC estimation, many studies have been carried out to investigate their estimation accuracy. In general, both satellite and receiver DCB values are relatively stable. Using 19 months GPS observations, Sardon and Zarraoa [14] concluded that GPS satellite biases were quite stable and the variations of satellite biases during 19 month periods were <3 TECU with a root mean square (RMS) of 0.5 TECU. For receiver biases, the changes over 19 months are within 6–10 TECU. Ciraolo *et al.* [4] showed that the intra-day variations of receiver DCB can reach 1.4–8.8 TECU and levelling process which translates the code delay to carrier phase observables can introduce errors up to 5.3 TECU. To assess estimation accuracy, Brunini and Azpilicueta [2] estimated receiver DCB using simulated ionosphere distributions under different locations and ionospheric conditions. Based on the simulation, the receiver DCB accuracy is within 2 TECU during low solar activity periods. However, in low latitudes and under strong solar activities, receiver DCB error can be >15 TECU. Having used GPS observation for 1 year in China, Zhang *et al.* [20] also demonstrated that the accuracy of receiver DCB estimation is location dependent. In mid-latitudes, the RMS value of receiver DCB is within 2 TECU. But the RMS value for low latitude receivers is around 3–4 TECU which can cause TEC estimation errors to 6–8 TECU.

In fact, the receiver DCB estimation errors are caused by many factors, such as GPS data quality, ionosphere model accuracy, data processing methods, etc. To further improve GPS receiver DCB estimation accuracy, we should understand more on what factors are the main limitations for estimating receiver DCB and how much affected these factors are. Brunini and Azpilicueta [1] used simulated ionosphere and co-located GPS receivers, trying to analyse the contribution of levelling error and model error to receiver DCB estimation accuracy. In this paper, we will examine a number of factors which affect receiver DCB estimation variations, such as receiver locations, different ionosphere models and data processing strategies, through a number of designed tests. In the next section of this paper, the method for receiver DCB estimation is briefly introduced. The details of the tests and results are presented in the section on ‘Analysis of factors affecting DCB estimation’. The conclusions and discussions are given in the last section.

## Global positioning system hardware DCB estimation method

The observation equations of dual frequency GPS pseudorange measurements can be expressed as [15]

$$P_1 = S + \frac{40.3}{f_1^2} E(z) + b^{s1} + b_{r1} + n_1 \quad (1)$$

$$P_2 = S + \frac{40.3}{f_2^2} E(z) + b^{s2} + b_{r2} + n_2 \quad (2)$$

where  $P_1$  and  $P_2$  are pseudorange measurements in  $L_1$  and  $L_2$  bands,  $S$  is the term not related to frequency, i.e. distance, tropospheric delay and clock errors,  $f_1$  and  $f_2$  are carrier frequencies in  $L_1$  and  $L_2$  bands,  $b^s$  and  $b_r$  are satellite and receiver biases respectively,  $E(z)$  is TEC along the signal pass, and  $n_1$  and  $n_2$  are measurement noises.

For ionosphere study, the geometry-free linear combination is normally formed to remove range related term

$$P_4 = \left( \frac{40.3}{f_1^2} - \frac{40.3}{f_2^2} \right) E(z) + \Delta b^s + \Delta b_r + n_4 \quad (3)$$

where  $\Delta b^s$  and  $\Delta b_r$  are the DCBs for satellite and receiver, and  $n_4$  is the noise term.

For a single-layer ionosphere model (as shown in Fig. 1), where  $z$  is the zenith distance at the receiver’s location,  $z'$  is the satellite’s zenith distance at the IPP and  $H$  is the height of the single layer. The slant TEC  $E(z)$  is commonly converted to the vertical TEC (VTEC)  $E_v$ , by a mapping function  $M(z)$

$$E(z) = M(z)E_v(x,y) \quad (4)$$

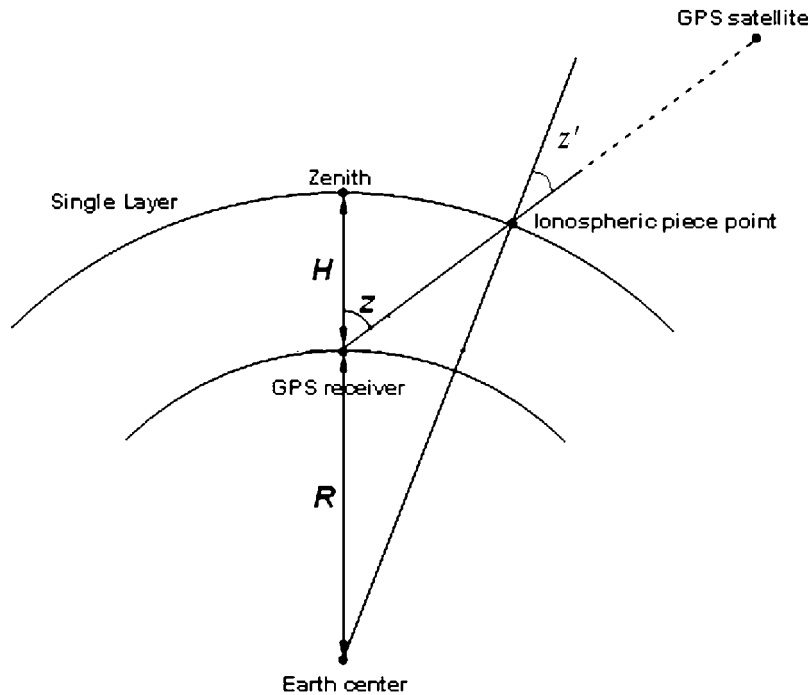
and

$$M(z) = \frac{1}{\cos z'} \quad (5)$$

where  $x$  and  $y$  are the coordinates of the IPP.

To estimate satellite and receiver DCBs, the VTEC  $E_v(x,y)$  is represented by a spatial function with a number of parameters to adjust its shape. Using GPS measurements from a number of receivers and over a period of time, the satellite and receiver DCBs, together with the parameters to represent VTEC spatial distribution, can be estimated by equation (3). From equation (3), it can be seen that the estimation accuracy of DCB values is determined by the noise level of GPS measurements, the correlation of DCB and the parameters in the function to represent VTEC, and the accuracy of the VTEC model. If the spatial function selected cannot model the spatial distribution of TEC precisely, it would cause DCB estimation errors and the increase in residual sizes.

Various functions have been suggested to model VTEC spatial distributions and most commonly used functions are the polynomial function [5], [7], and spherical harmonic (SH) expansion [16]. Sekido *et al.* [17] applied a two-dimensional VTEC model which is expressed by the product of independent longitudinal and latitudinal functions. When different models are selected, the DCB estimation accuracy can be affected. Even with the same model, selecting different degrees and orders will give totally different models. Using the SH function, as an example, the spatial resolutions are significantly different when different degrees and orders are selected. Equations (6) and (7) give the general forms of the SH function and the polynomial function respectively.



1 Single-layer model for the ionosphere [15]

$$E(\beta, S) = \sum_{n=0}^{n_{max}} \sum_{m=0}^n \tilde{p}_{nm}(\sin \beta) [c_{nm} \cos(ms) + s_{nm}(ms)] \quad (6)$$

where  $\beta$  is the geographic latitude of the intersection point of the light of sight with the single layer,  $S = \lambda - \lambda_0$  is the sun-fixed longitude of the IPP,  $\lambda$  is the longitude of the IPP,  $\lambda_0$  is the longitude of the sun,  $n_{max}$  is maximum degree of the SH expansion,  $\tilde{p}_{max}$  is the normalised associated Legendre functions of degree  $n$  and order  $m$ , and  $c_{max}$  and  $s_{nm}$  are the unknown SH coefficients and global ionosphere map parameter respectively.

And

$$E(\beta, S) = \sum_{n=0}^{n_{max}} \sum_{m=0}^{m_{max}} E_{nm}(\beta - \beta_0)^n (s - s_0)^m \quad (7)$$

where  $n_{max}$  and  $m_{max}$  are the maximum degrees of the two-dimensional Taylor series expansion in latitude  $\beta$  and in longitude  $s$ ,  $E_{nm}$  is the TEC coefficient of the Taylor series, i.e. the local ionosphere model parameters to be estimated,  $\beta_0$  and  $s_0$  are the coordinates of the origin of the development,  $\beta$  is the geographic latitude of the IPP and  $S$  is the sun-fixed longitude of the IPP.

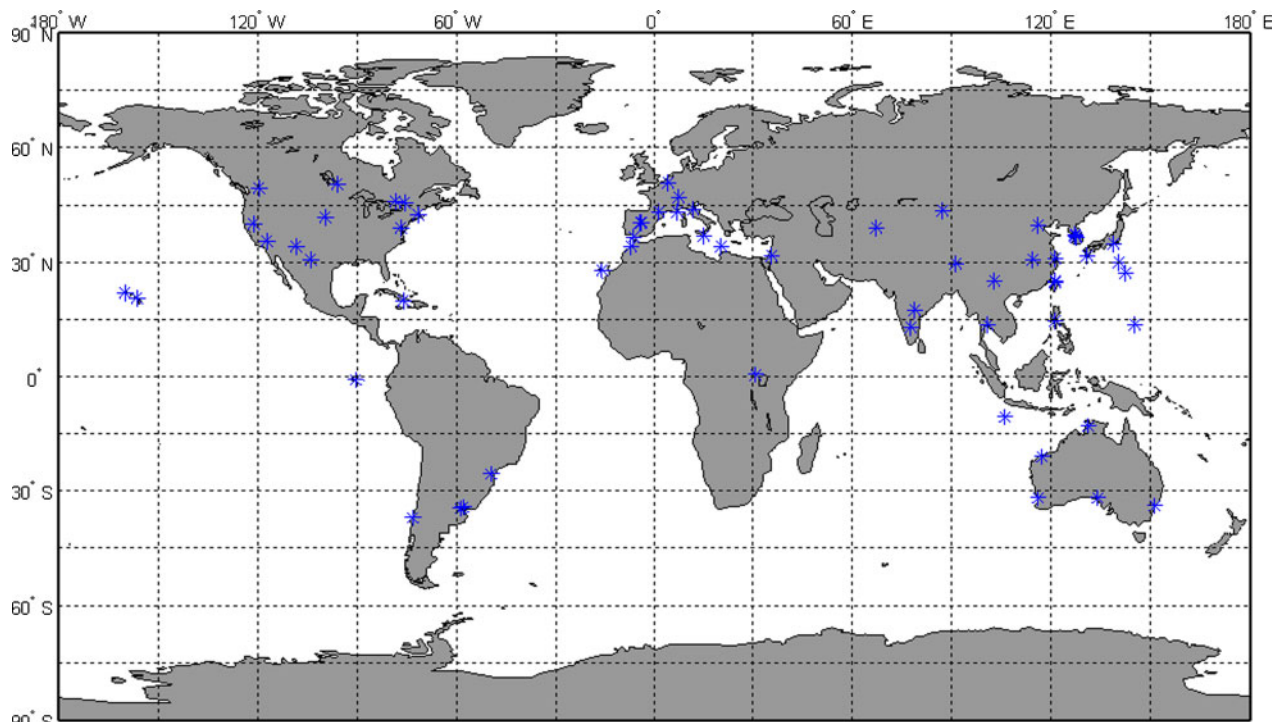
The SH function with different degrees and orders has been suggested for global and regional ionosphere model and even to the so called station-specific TEC model [7]. Ideally, with higher degrees and orders, the SH model will be better to represent the spatial distribution of VTEC. However, the number of parameters to be estimated increases dramatically with higher degrees and orders of SH function. The spatial distribution of GPS measurements is also a limitation. In practice, the degrees and orders of the SH function should be selected to correspond to the density of GPS network and to control data processing complexity. For example, the Center for Orbit Determination in Europe (CODE) has generated the global ionosphere model (GIM) since 1996. The GIM produced by CODE is modelled with 256 coefficients of SH expansion up to  $15^\circ$  and 15 orders

for the global TEC representation [18]. While for station-specific model, a  $4 \times 4$  SH model is adopted by CODE [15]. With more than 100 GPS stations, the South American regional ionosphere model (La Plate Ionosphere Model or LPIM) adopted an SH expansion with degrees and orders to 15 [1]. Ping et al. [12] even applied  $60 \times 60$  SH expansion to develop an ionosphere model for Japan, using more than 1000 GPS stations in the region.

**Analysis of factors affecting DCB estimation**

In this study, we are mainly interested in the receiver DCB estimation accuracy. Therefore, the satellite DCB values are adopted from the IGS values (<http://igs.cb.jpl.nasa.gov/>). A number of tests are designed to investigate various factors which affect the estimation accuracy of receiver DCBs. The first group of tests tries to analyse the effects with different VTEC models and locations. The second group of tests intends to investigate the effects of different data processing strategies, such as pseudorange smoothing and elevation cut-off angles. As there are no more accurate DCB values for comparison, in this study, the daily variations of the estimated receiver DCB values are used to quantify the quality of the estimation. For IGS stations used in this study, the receiver DCB values from the IGS data processing centre are also used for comparison. The IGS global VTEC maps are combined by four IAACs analysis centres, CODE, ESA, JPL and UPC. The evaluation of the different global VTEC maps is provided by UPC, based on how they are able to reproduce observed STEC variation. The IGS DCB values are provided by these centres in a similar way [9].

The Bernese software V5.0 is used to process GPS data in this study. To minimise the impact of multipath and systemic noise of code observation, the smoothing code observations of dual frequency GPS data are used for most of the tests to estimate the receiver DCB values,



**2 The IGS stations used for the study**

unless it is specified. The details for the smoothing code observation can refer to [19].

### Global positioning system network with a global model

This test serves two purposes. The first purpose is to evaluate the accuracy of the software used and data processing method adopted in the study, by comparing our receiver DCB results with those published by IGS. The second purpose of the test is to examine the dependence of receiver DCB estimation accuracy on different locations. In the test, we select globally distributed 60 IGS GPS stations (as shown in Fig. 2). The continued 30 days of GPS data (day of year 171–200 of 2009) from the selected 60 stations are used in the test. During this period, the geomagnetic activity was quiet with the Dst geomagnetic index greater than  $\sim 50$  nano-Tesla (nT) (<http://swdcwww.kugi.kyoto-u.ac.jp/dstdir/finalprov.html>). The data sampling rate is 30 s and the elevation cut-off angle of  $30^\circ$  is adopted.

The SH expansion function is used for VTEC model with degrees and orders  $12 \times 8$ . Firstly, we calculate daily mean receiver DCB values for each station for all 30 days. Then the estimated receiver DCB values are compared with those published by IGS (<ftp://cddis.gsfc.nasa.gov/pub/gps/products/ionex>). For all 60 stations, the mean of difference for each station for the whole month ranges from  $-4.6$  to  $5.3$  TECU, with a mean value of  $-0.8$  TECU and RMS of  $2.5$  TECU for all 60 stations. Figure 3 illustrates an example of station TCMS in Taiwan. It can be seen that except a bias of  $1.2$  TECU, the daily variations by IGS and our estimated are very similar. Considering that IGS receiver DCB errors are in the range of  $3\text{--}4$  TECU [17], our estimated results are compatible with IGS published DCB values.

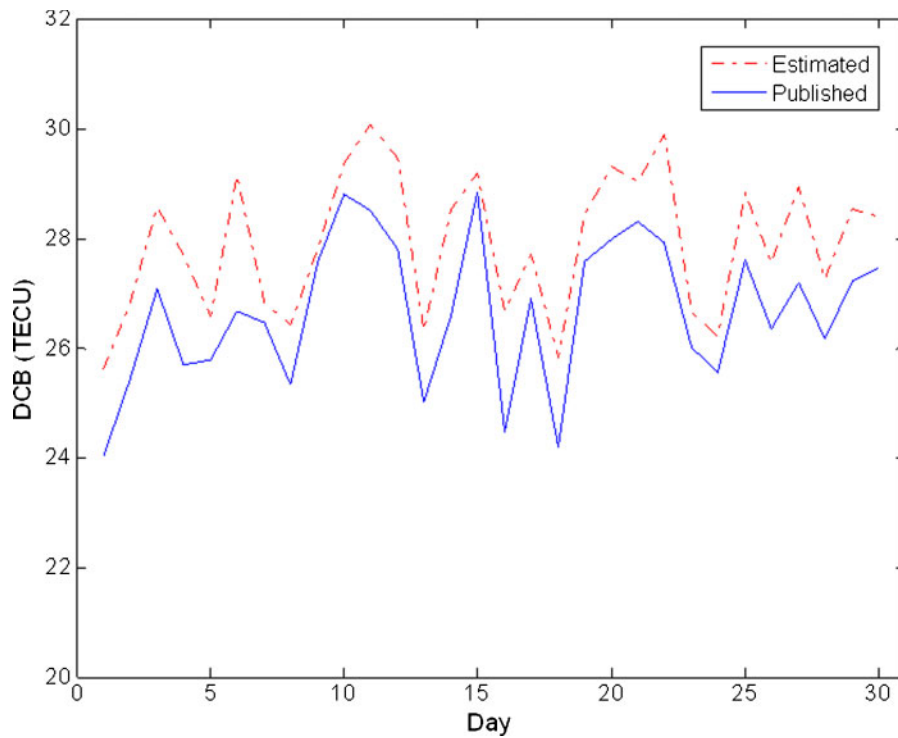
Then for each receiver, we calculated the maximum DCB variations (maximum value–minimum value) and RMS value for the 30-day period. As an example,

Table 1 gives the daily variation range and RMS of receiver DCB for all stations in America area. In the north hemisphere middle latitude (latitudes  $30\text{--}50^\circ$ ), the daily variations range from  $2.0$  to  $3.6$  TECU and the RMS ranges from  $0.5$  to  $0.9$  TECU, except NRC1. For low latitudes ( $\pm 20^\circ$ ), the variations are much larger, with the daily variations range from  $5.5$  to  $5.8$  TECU and the RMS ranges from  $1.0$  to  $1.4$  TECU. This result confirms the studies of Sardon and Zarraoa [14] and Brunini and Azpilicueta [1] that receiver DCB estimation accuracy is worse in low latitudes. As the ionosphere spatial gradients in low latitudes are much larger than those in middle latitudes [3], the same SH model ( $12 \times 8$ ) is fitted with ionosphere VTEC spatial variations much better in middle latitudes than in low latitude. As a result, the estimation accuracy of receiver DCB is lower in low latitude region. Also, we can notice that the DCB variations in south hemisphere middle latitudes are also worse than those from north hemisphere. This may be because the number of stations that we selected in the south hemisphere is much less. Also in Table 1, we list the mean differences of the estimated receiver DCB and corresponding IGS values, which are in the range from  $0.01$  to  $-4.6$  TECU.

### The global versus the station-specific SH models

In this test, we try to investigate receiver DCB estimation differences between a global solution (all 60 stations) and a station-specific solution (one station). For the station-specific solution, we adopt a  $5 \times 5$  SH model. Table 2 shows a number of selected stations in Asia area. It can be seen that the mean differences are in the range from  $-1.2$  to  $5.4$  TECU, while the maximum differences can reach  $14$  TECU at KUNM station. Again, the differences are significantly larger in low latitudes.

Also, we calculated maximum daily variations and RMS values of receiver DCB estimation for each station



### 3 The comparison between calculated biases and IGS published DCBs of station TCMS

for the 30-day period, using both models. The results are shown in Table 3. It can be seen for all stations, the DCB values are much stable with the global solution.

#### Comparison of Taylor and SH model for regional network

In this test, we try to compare the DCB estimations from two completely different types of models. In this test, two commonly used models, the polynomial function and SH model, are selected for the tests. In the test,  $5 \times 5^\circ$  and order SH model and  $2 \times 2^\circ$  of latitude and hour angle polynomial function model are adopted. Three IGS stations in middle latitudes (GOLD, JPLM and PIN1) with a cover region of roughly  $200 \times 200$  km are selected for the test. Table 4 shows the 30-day DCB estimation variations for each method. It can be seen

that the variations of the estimated DCB values for the two models are quite similar with RMS values all  $<1.6$  TECU. However, the estimated mean DCB values over this 30-day test period are significantly different (as shown in Table 5). The mean DCB value estimated by the polynomial function model is around 5 TECU larger than that by the SH model. This shows again that with different VTEC models, the estimated DCB can be significantly different.

#### The DCB behaviour and the distance between stations

As discussed in the previous sections, the DCB daily variations depend on how well the model is fitted with the VTEC spatial distributions. Therefore, if two stations are closed, the DCB variations should be highly

**Table 1** The daily variation range and RMS of receiver DCB of America area

Station name	DCB maximum/ TECU	DCB minimum/ TECU	Maximum daily variation/TECU	RMS/ TECU	Mean difference to IGS/TECU	Station latitude/°
DUBO	14.25	12.25	2.00	0.559	-4.24	50.3
DRAO	48.22	44.56	3.66	0.883	-4.40	49.3
ALGO	11.47	8.19	3.28	0.969	-4.12	46.0
NRC1	-45.88	-50.92	5.04	1.267	-3.82	45.5
WES2	-6.19	-8.36	2.17	0.616	-3.73	42.6
NLIB	21.75	18.19	3.56	0.867	-3.58	41.8
QUIN	-21.67	-23.94	2.27	0.752	-4.37	40.0
GODE	-8.58	-11.01	2.43	0.626	-3.63	39.0
GOLD	-17.98	-21.01	3.03	0.873	-4.61	35.4
PIE1	-9.79	-12.48	2.69	0.725	-3.53	34.3
MDO1	-5.26	-7.86	2.60	0.810	-3.75	30.7
KOKB	-14.44	-20.24	5.80	1.400	-2.02	22.1
MAUI	-20.04	-25.53	5.49	1.370	-2.05	20.7
SCUB	-29.74	-33.58	3.84	1.066	-1.89	20.0
GLPS	-3.34	-7.95	4.61	1.282	2.03	-0.7
UFPR	59.89	54.54	5.35	1.117	3.17	-25.4
LPGS	39.93	33.97	5.96	1.078	0.66	-34.0
BUE1	-16.40	-22.34	5.94	1.086	0.80	-34.6
CONZ	24.36	17.99	6.37	1.104	0.01	-36.8

**Table 2 The DCB value differences with global and station-specific SH models**

Station name	Maximum difference of two ionosphere models/TECU	Mean difference of two ionosphere models/TECU	Geographic latitude/°
BJFS	-2.5	-0.3	39.6
SUWN	-5.9	-1.2	37.3
OSN1	-5.2	0.7	37.1
DAEJ	-4.6	-0.7	36.4
AIRA	-3.7	0.5	31.8
SHAO	3.2	0.8	31.1
WUHN	5.0	1.9	30.5
LHAZ	4.6	0.8	29.7
KUNM	-14.3	1.6	25.0
TCMS	5.1	3.0	24.8
TNML	4.9	3.0	24.8
PIMO	11.0	5.4	14.6
CUSV	8.8	3.6	13.7

**Table 3 The RMS and maximum daily variation of DCB with global and station-specific SH model**

Station name	Model type	RMS/TECU	Maximum daily variation/TECU	Geographic latitude/°
BJFS	Global	1.2	4.4	39.6
	Station	2.1	6.3	
SUWM	Global	1.3	4.5	37.3
	Station	1.8	9.0	
OSN1	Global	1.3	5.6	37.1
	Station	2.0	9.6	
DAEJ	Global	1.0	4.1	36.4
	Station	1.3	5.3	
AIRA	Global	1.0	4.1	31.8
	Station	1.8	7.6	
SHAO	Global	0.9	3.3	31.1
	Station	1.6	6.4	
WUHN	Global	0.9	3.6	30.5
	Station	2.1	7.0	
LHAZ	Global	1.3	6.6	29.7
	Station	2.2	9.9	
KUNM	Global	2.2	9.3	25.0
	Station	4.3	23.0	
TCMS	Global	1.3	4.5	24.8
	Station	1.9	7.1	
TNML	Global	1.4	4.9	24.8
	Station	2.0	7.1	
PIMO	Global	0.9	3.2	14.6
	Station	2.4	10.2	
CUSV	Global	1.2	5.0	13.7
	Station	2.6	9.7	

**Table 4 The RMS and maximum daily variation of DCB with polynomial and regional SH models**

Station name	Model type	RMS/TECU	Maximum daily variation/TECU	Geographic latitude/°
GOLD	Taylor	0.49	2.12	35.42
	Regional SH	0.52	2.32	
JPLM	Taylor	1.58	7.45	34.20
	Regional SH	1.48	7.23	
PIN1	Taylor	0.39	1.59	33.61
	Regional SH	0.72	3.44	

**Table 5 The DCB value differences with polynomial and regional SH models**

Station name	Taylor 30 days average/TECU	Regional SH 30 days average/TECU	Maximum difference between different ionosphere models/TECU	Mean of difference of different ionosphere models/TECU
GOLD	-11.79	-17.44	7.28	5.6
JPLM	24.90	20.33	5.87	4.6
PIN1	-11.51	-15.82	5.62	4.5

correlated and the correlation will be reduced if the distance between two stations increases. In this test, we selected a number of stations in Asia region which have similar latitudes or longitudes, with distances to station TCMS from 5 to 3000 km. Then we estimate daily receiver DCB values for each station and calculate the correlation coefficients between TCMS and other stations. The results are shown in Tables 6 and 7. As shown in Tables 6 and 7, when two stations (TCMS and TNML) are very close (5 km), the correlation is very high, with the correlation coefficient of 0.98. This means that the DCB variation trends of these two stations are almost the same. On the other hand, with the increase in distance, the correlations decrease with distance. This test, from another point of view, demonstrates that estimated DCB variations are closely linked to the fitness of the ionospheric model to the real VTEC spatial distributions. When the two stations are closed, if the degree of the model fitness is the same, the DCB variations are also similar.

### Comparison of DCB variations with the size of residuals

As discussed in the Section on ‘Global positioning system hardware DCB estimation method’, if the ionospheric models used cannot present the VTEC spatial variations well, it will increase DCB estimation errors and at the same time, increase the size of residuals. Thus, large DCB variations should be correlated with the increase in residual size. In this test, the residual size is presented by the standard deviation of the residuals. A sample’s results are given in Table 8. In the second column of the table, we calculated the correlation coefficients between the DCB variations and the standard deviation of residuals. It

seems that there were not strong correlations between these two data series for all stations, as the coefficients are in the range of 0.5–0.6. However, if we only consider large DCB variations by filtering out DCB variations within the standard deviation and calculate the correlation coefficients with those large DCB variations, we find that the correlations are very strong for all stations with the range of 0.71–0.95 (as shown in the third column of the table). Again, this test demonstrates that the importance of ionospheric model accuracy is the key factor for better receiver DCB estimation.

### The difference of DCB between smooth and non-smooth observations

In GPS data processing for TEC estimation, carrier smoothed pseudorange measurements are commonly used for reducing the measurement noise and multipath. In this test, we try to evaluate the effects of pseudorange smoothing on receiver DCB estimation. We simply recalculate the receiver DCB values without using smoothing and then compare them with the results with smoothing. The results are given in Table 9. From the table, it can be seen that the mean differences are in the range of 2–4 TECU, with the maximum differences of 4.3–6.8 TECU.

Also, we compared the estimation results with the corresponding IGS values (as shown in Table 10). Compared with IGS values, the mean differences are between 0.1 and 2.1 TECU and the maximum differences are in the range from –3.5 to 3.4 TECU, with the smoothed pseudorange. Without smoothing, the maximum difference can reach to 6.6 TECU. Thus, the receiver DCB estimation accuracy is higher with smoothed pseudorange.

**Table 6** The correlation coefficient for different distances of stations (similar latitudes)

Station name	Latitude	Longitude	Distance to TCMS/km	Correlation coefficient of DCB daily variation
TCMS	24.8	120.9	0	...
TNML	24.8	120.9	5	0.977
WUHN	30.5	114.3	910	0.843
KUNM	25.0	102.7	1830	0.514
LHAZ	29.5	91.1	2973	0.238

**Table 7** The correlation coefficient for different distances of stations (similar longitude)

Station	Latitude	Longitude	Distance to TCMS/km)	Correlation coefficient of DCB daily variation
TCMS	24.8	120.9	0	...
SHAO	31.1	121.2	698	0.894
PIMO	14.5	121.1	1123	0.541
DAEJ	36.3	127.4	1420	0.484

**Table 8** The correlation coefficient of daily variation of DCB values and their residual

Station name	Correlation coefficient	After filtering	Geographic latitude/°
BJFS	0.62	0.95	39.6
DAEJ	0.59	0.78	36.4
WUHN	0.60	0.85	30.5
LHAZ	0.54	0.93	29.7
KUNM	0.55	0.86	25.0
TCMS	0.55	0.73	24.8
TNML	0.57	0.76	24.8
XMIS	0.56	0.71	–10.7

**Table 9** The difference of DCB values calculated from smooth and non-smooth GPS observations

Station name	Maximum difference between smooth and non-smooth/TECU	Mean of difference between smooth and non-smooth/TECU	Station latitude/°
BJFS	6.8	2.6	39.6
OSN1	4.9	2.3	37.1
DAEJ	5.3	2.0	36.4
WUHN	4.8	3.5	30.5
LHAZ	4.3	3.3	29.7
KUNM	4.9	3.7	25.0
TCMS	4.9	3.8	24.8
TNML	6.5	4.0	24.8
PIMO	5.1	3.8	14.6

**Table 10** The difference of DCB values calculated from smooth and non-smooth GPS observations compared with IGS results

Station name	Smooth compared with IGS/TECU		Non-smooth compared with IGS/TECU		Station latitude/°
	Maximum difference	Mean difference	Maximum difference	Mean difference	
BJFS	-1.2	-0.1	6.6	2.7	39.6
OSN1	-1.4	-0.5	5.0	2.7	37.1
DAEJ	-1.4	-0.5	4.4	2.5	36.4
WUHN	1.7	0.7	3.7	2.8	30.5
LHAZ	1.3	0.4	3.8	2.9	29.7
KUNM	-3.5	0.0	5.2	3.7	25.0
TCMS	2.5	1.3	3.3	2.5	24.8
TNML	2.9	1.4	4.1	2.6	24.8
PIMO	3.4	2.1	2.8	1.7	14.6

### The comparison of different cut-off angles

In GPS data processing for TEC estimation, the satellite elevation cut-off angles are normally set much higher than for positioning, i.e. 20 or 30°. The reason behind it is to try to reduce the effects of multipath. Is this true, as most GPS permanent stations are located at the places with clear sky? In this test, we calculate receiver DCBs with different cut-off angles, from 10 to 30°. The sample results are shown in Table 11. From our test, we can see that the effects of cut-off angle on receiver DCB estimation are very limited, with the maximum difference <0.4 TECU.

### Discussion and conclusions

In this study, we have designed a number of tests, trying to evaluate various factors affecting GPS receiver DCB estimation accuracy. The tests are divided into two

groups. The tests of the first group try to analyse the effects of ionospheric models on receiver DCB estimation accuracy:

- (i) The receiver DCB estimation accuracy is location and receiver density dependent; in low latitude regions, the estimation accuracy is lower, because TEC distributions in low latitudes are much more complicated than those in mid-latitudes.
- (ii) Using different degrees and orders SH models for the same receiver, we find that the estimated DCB values can differ in a range of -2.5–14.3 TECU, with the mean of differences from -0.3 to 5.4 TECU. Again, the larger fluctuation happened at the low latitude stations.
- (iii) The DCB estimations for a small regional network (200 × 200 km) from both the Taylor series and SH models are compared. The results show that the mean difference of the DCB

**Table 11** DCB differences between different cut-off angles/TECU

Station name	10° versus 30° (maximum)	10° versus 30° (mean)	20° versus 30° (maximum)	20° versus 30° (mean)
BJFS	0.18	0.096	0.13	0.054
DAEJ	0.157	0.095	0.128	0.105
WUHN	0.408	0.210	0.302	0.153
LHAZ	0.188	-0.076	0.106	-0.201
KUNM	0.160	-0.027	0.171	-0.045
TCMS	0.211	0.080	0.137	0.048
TNML	0.165	0.031	0.131	0.033
PIMO	0.399	0.274	0.294	0.198
XMIS	0.185	-0.039	0.126	-0.015
DUBO	0.200	-0.13	0.137	-0.081
DRAO	0.128	-0.052	0.068	-0.022
NRC1	0.049	0.006	0.051	0.016
NLIB	0.134	-0.035	0.106	-0.050
MOD1	0.123	0.071	0.094	0.064
KOKB	0.217	0.055	0.146	0.042
SCUB	0.128	0.036	0.114	0.026
LPGS	0.111	-0.056	0.071	-0.013

estimations from the two models can reach over 5 TECU.

- (iv) Larger DCB estimation variations are strongly correlated to residual changes. This indicates that the accuracy of the ionospheric model used in equation (3) plays an important role in receiver DCB estimation.
- (v) The daily variation of the receiver DCB is highly correlated with the receiver location. In the neighbourhood sites, even with different types of receivers, the estimated DCB values present with a high correlation. The correlation coefficient decreases while the distance between two sites increases. This, from another point of view, indicates that the DCB estimation is linked to the model accuracy.

The tests of the second group tests investigate the effects of DCB estimation due to data processing:

- (i) The DCB estimations from the smoothing and non-smoothing GPS observations are compared. It shows that the difference reaches up to 6.8 TECU.
- (ii) In most GPS data processing for ionospheric delay estimation, the elevation cut-off angle is normally selected significantly higher than that for positioning. However, in our test, we find that the elevation cut-off angle does not affect receiver DCB estimation very much, less than 0.4 TECU.

Based on this study, we can conclude:

1. The most important factor affecting GPS ionosphere estimation accuracy is the mathematical models used to describe the spatial distribution of VTEC. Using functions with higher degrees and orders can fit VTEC better, but it is restricted by the density of GPS network. Thus to improve GPS ionosphere estimation accuracy, it is important to develop empirical functions which can fit VTEC distribution better, at the same time, with less parameters to be adjusted.

2. The GPS data processing methods also affect GPS receiver DCB estimation. Carrier smoothing or levelling process should be used in data processing. Changing elevation cut-off angle will not affect receiver DCB estimation significantly.

3. Many studies have demonstrated that the daily variations of receiver DCB can be significant [1],[4]. In this study, we suggested that most of such DCB variations are due to estimation errors. Further studies are required on how to distinguish the real receiver DCB changes and the estimation errors.

## Acknowledgement

This study is partially supported by the Hong Kong CERG research fund (PolyU 5131/10E).

## References

1. Brunini, C. and Azpilicueta, F., 2009. Accuracy Assessment of the GPS-based Slant Total Electron Content. *Journal of Geodesy*, 83(8): 773–785.
2. Brunini, C. and Azpilicueta, F., 2010. GPS Slant Total Electron Content Accuracy Using the Single Layer Model Under Different Geomagnetic Regions and Ionospheric Conditions. *Journal of Geodesy*, 84: 293–304.
3. Chen, W., Gao, S., Hu C., Chen, Y. and Ding, X., 2008. Effects of Ionospheric Disturbances on GPS Observation in Low Latitude Area. *GPS Solution*, 12: 33–41.
4. Ciraolo, L., Azpilicueta, F., Brunini, C., Meza, A. and Radicella, S. M., 2007. Calibration Errors on Experimental Slant Total Electron Content (TEC) Determined with GPS. *Journal of Geodesy*, 81: 111–120.
5. Coco, D. S., Dahlke, S. R. and Cynch, J. R., 1991. Variability of GPS Satellite Differential Group Delay Biases, *IEEE Transactions on Aerospace and Electronics Systems*, 27(6): 931–938.
6. Coster, A. and Komjathy, A., 2008. Space Weather and the Global Positioning System, *Space Weather*, 6: S06D04, doi:10.1029/2008SW000400.
7. Dach, R., Hugentobler, U., Fridez, P. and Meindl, M. (eds.). 2007. Bernese GPS Software Version 5.0. Astronomical Institute University of Bern, Bern.
8. Dyrud, L., Jovancevic, A., Brown, A., Wilson, D. and Ganguly, S., 2008. Ionospheric Measurement with GPS: Receiver Techniques and Methods. *Radio Science*, 43: R56002, doi:10.1029/2007RS003770.
9. Hernandez-Pajares, M., Juan, J. M., Sanz, J., Orus, R., Garcia-Rigo, A., Feltens, J., Komjathy, A., Chaer, S. C. and Krankowski, A., 2009. The IGS VTEC Maps: A Reliable Source of Ionospheric Information Since 1998. *Journal of Geodesy*, 83: 263–275.
10. Lunt, N., Kersley, L., Bishop, G. J., Mazzella, A. J. and Bailey, G., 1999. The effect of Protonosphere on the Estimation of GPS Total Electron Content: Validation Using Model Simulation. *Radio Science*, 34(5): 1261–1271
11. Mannucci, A. J., Wilson, B. D., Yuan, D. N., Ho, C. H. and Lindqwister, U. J., 1998. A Global Mapping Technique for GPS-derived Ionospheric Total Electron Content Measurements. *Radio Science*, 33: 565–582.
12. Ping, J., Kono, Y., Matsumoto, K., Otsuka, Y., Sauto, A., Shum, C., Heki, K. and Kawano, N., 2002. Regional, Ionosphere Map Over Japanese Islands. *Earth Planets Space*, 54: e12–e16.
13. Sardon, E., Rius, A. and Zarraoa, N., 1994. Estimation of the Transmitter and Receiver Differential Biases and the Ionospheric Total Electron Content from Global Positioning System Observations. *Raido Science*, 29: 577–586.
14. Sardon, E. and Zarraoa, N., 1997. Estimation of Total Electron-Content Using GPS Data: How Stable Are the Differential Satellite and Receiver Instrumental Biases. *Radio Science*, 32: 1899–1910.
15. Schaer, S., 1999. Mapping and Predicting the Earth's Ionosphere Using the Global Positioning System. *PhD Thesis*, Bern University, Switzerland.
16. Schaer, S., Beutler, G., Mervart, L., Rothacher, M. and Wild, U., 1995. Global and Regional Ionosphere Models Using the GPS Double Difference Phase Observable. *Proceedings of the IGS Workshop on Special Topics and New Directions*, Potsdam, Germany, 15–17 May: pp. 77–92.
17. Sekido, M., Kondo, T., Kawai, E. and Imae, M., 2003. Evaluation of GPS-based Ionospheric TEC Map by Comparing with VLBI Data. *Raido Science*, 38(4): 1069, doi:10.1029/2000RS002620.
18. Sekido, M., Kondo, T., Kawai, E. and Imae, M., 2004. Evaluation of Global Ionosphere TEC by Comparison with VLBI Data. *Proceedings of the International VLBI Service for Geodesy and Astrometry 2004 General Meeting*. Ottawa, Canada, 9–11 February; 427. <http://ivscc.gsfc.nasa.gov>.
19. Springer, T. A., 1999. Modeling and Validating Orbits and Clocks Using the Global Positioning System, *PhD Thesis*, Astronomical Institute, University of Berne, Switzerland.
20. Zhang, D. H., Zhang, W., Li, Q., Shi, L. Q. and Xiao, Z., 2010. Accuracy Analysis of the GPS Instrumental Bias Estimated from Observations in Middle and Low Latitudes. *Annales Geophysicae*, 28: 1571–1580.